ISSN 1070-3284, Russian Journal of Coordination Chemistry, 2016, Vol. 42, No. 6, pp. 385–391. © Pleiades Publishing, Ltd., 2016.

New Ni(II) and Co(II) Coordination Compounds Construction from the Ditopic 1,2,3-Triazol-Based Aromatic Heterocyclic Polycarboxylic Ligand[1]

Z. Zhou[a], W. Q. Zhang[a], R. R. Bian[a], C. X. Lan[a], W. Gu[b, c], X. Liu[b, c], *, and S. Y. Liao[a], *

[a] *Department of Applied Chemistry, Tianjin University of Technology, Tianjin, 300384 P.R. China*
[b] *Department of Chemistry, Nankai University, Tianjin, 300071 P.R. China*
[c] *Collaborative Innovation Center of Chemical Science and Engineering, Tianjin, 300071 P.R. China*
**e-mail: 18202587221@163.com; liuxin64@nankai.edu.cn*

Received July 10, 2015

Abstract—Mononuclear compound **I** ($[Co(Ptia)_2(H_2O)_4] \cdot H_2O$) and 1D chain compound **II** ($[Ni_4(Cptia)_4(H_2O)_{12}]_\infty$) have been constructed from the new ditopic 1,2,3-trazol-based aromatic heterocyclic carboxylic ligand, 4-(4-carboxy-1*H*-1,2,3-triazol-1-yl) benzoic acid) (H_2Cptia), under different pH conditions by using the hydrothermal method. Their structure was characterized by single crystal X-ray diffraction (CIF files CCDC nos. 1409531 (**I**) and 1409531 (**II**)), IR spectra, and elemental analysis. Compound **I** is a mononuclear compound. In **II**, two sets of parallel arrangement 1D chains orient in different directions. The results of their magnetic measurements display the antiferromagnetic interaction exists among the paramagnetic ions.

DOI: 10.1134/S1070328416060099

INTRODUCTION

Design and synthesis of molecular-based magnetic materials have always been the hotspot research fields for chemical workers. On the premise of selection the appropriate spin carrier, seeking functional organic module, and controlling the assembly conditions are the key issues for regulating magnetic interactions to obtain the coordination compounds with good magnetic properties [1–5]. The spin carriers of Co(II), and Ni(II) is the good candidates for constructing molecular-based magnetism [6–11]. Because four-coordinated and six-coordinated Co(II), and Ni(II) can not only coordinate with the N donor, but also with the O donor, the aromatic heterocyclic carboxylic ligands were extensively used to construct the magnetic coordination compounds with novel structure [12–16]. A large number of the reported heterocyclic complexes mainly focus on the pyridine, imidazole, and 1,2,4-triazol substituted aromatic carboxylic ligand [17–20]. In recent years, the click reaction paved the way for us to design and synthesize the 1,2,3-triazol substituted aromatic polycarboxylic ligand [21, 22]. In order to gain the low dimensional complexes and reduce the magnetic coupling among the molecules and chains, the tunable structure of ditopic 1,2,3-triazol substituted aromatic carboxylic ligand has been designed and synthesized. The routine for synthesis ligand H_2Cptia is given below:

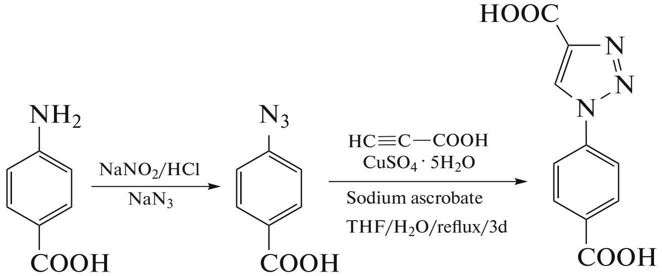

H_2Cptia

---

[1] The article is published in the original.

With this ligand, mononuclear compound $[Co(Ptia)_2(H_2O)_4] \cdot H_2O$ (**I**) and 1D chains compound $[Ni_4(Cptia)_4(H_2O)_{12}]_\infty$ (**II**), where H_2Ptia = 4-(1*H*-1,2,3-triazol-1-yl) benzoic acid, H_2Cptia = 4-(4-carboxy-1*H*-1,2,3-triazol-1-yl) benzoic acid), has been synthesized through the hydrothermal method.

EXPERIMENTAL

Materials and methods. The reagents and solvents were obtained from commercial sources and used as received without further purification. Elemental analyses were determined on a Perkin-Elmer PE 2400 CHNS/O analyzer. IR spectra (KBr pellets) were recorded on a Perkin-Elmer spectrometer in the range 4000–400 cm^{-1}. Temperature magnetic measurements were carried out on a SQUID-MPMS-XL magnetometer. Diamagnetic corrections were made with Pascal's constants.

Synthesis of H_2Cptia. 4-Azidobenzoic acid (1.63 g, 10 mmol) (being synthesized according to the literature [23]), propolic acid (0.62 mL, 12 mmol), and the mixture solvent of THF and H_2O (v : v, 1 : 1) was added into the 250 mL rottom flask and stirred for 10 min. Then sodium aseorbate (0.25 g, 1 mmol) and $CuSO_4 \cdot 5H_2O$ (0.025 g, 0.01 mmol) was addded. After the reaction mixture was refluxed for 24 h, the ice water was added and the white precipitate appeared. The precipitate was washed with deionized water for several times and dried in the air. The yeild of H_2Cptia was 1.85 g (85%) based on 4-azidobenzoic acid.

^{1}H NMR (300 MHz; DMSO-d_6; δ, ppm) 7.20 (d., 2H), 7.94 (d., 2H), 8.11 (s., 1H).

Synthesis of $[Co(Ptia)_2(H_2O)_4] \cdot H_2O$ (I). $Co(NO_3)_2 \cdot 6H_2O$ (0.0291 g, 0.01 mmol), H_2Cptia (0.233 g, 0.01 mmol) whose pH was 2, and 8 mL deionized water were placed in a 10 mL Teflon-linear autoclave. The reaction mixture was heated to 160°C in an oven for 24 h, and then cooled down to room temperature at a rate of 2°C/min. Red block crystals suitable for X-ray structural analysis were obtained with a yield of 0.0157 g (30%) based on $Co(NO_3)_2 \cdot 6H_2O$.

For $C_{18}H_{22}N_6O_9Co$ (*M* = 525.35)

anal. calcd., %:	C, 28.57;	H, 3.05;	N, 9.09.
Found, %:	C, 28.60;	H, 3.04;	N, 9.10.

IR (KBr pellets; ν, cm^{-1}): 3358 w, 1620 s, 1566 s, 1438 w, 1380 w, 1222 w, 1121 s, 919 s, 853 s, 730 s, 600 s.

Synthesis of $[Ni_4(Cptia)_4(H_2O)_{12}]_\infty$ (II). $Ni(NO_3)_2 \cdot 6H_2O$ (0.0290 g, 0.01 mmol), H_2Cptia (0.233 g, 0.01 mmol) whose pH was adjusted to 5 by adding NaOH (0.0040 g, 0.01 mmol), and 8 mL deionized water were placed in a 10 mL Teflon-linear autoclave. The reaction mixture was heated to 160°C in an oven for 24 h, and then cooled down to room temperature at a rate of 2°C/min. Green block crystals suitable for X-ray structural analysis were obtained with a yield of 0.034 g (40%) based on $Ni(NO_3)_2 \cdot 6H_2O$.

For $C_{40}H_{44}N_{12}O_{28}Ni_4$ (*M* = 1375.71)

anal. calcd., %:	C, 34.92;	H, 3.22;	N, 12.22.
Found, %:	C, 34.60;	H, 3.19;	N, 12.23.

IR (KBr pellets; ν, cm^{-1}): 3360 w, 1624 s, 1565 s, 1437 w, 1383 w, 1223 s, 1118 s, 920 s, 851 s, 732 s, 602 s.

X-ray structure determination. Diffraction data for complexes **I** and **II** were collected with a Bruker SMART APEX CCD instrument with graphite monochromatic MoK_α radiation (λ = 0.71073 Å). The data were collected at 293(2) K. The absorption corrections were made by multi-scan methods. The structure was solved by charge flipping methods with the program Olex2 and refined by full-matrix least-squares methods on all F^2 data with Olex2. The non-hydrogen atoms were refined anisotropically. Hydrogen atoms of water molecules were located in a different Fourier map and refined isotropically in the final refinement cycles. Other hydrogen atoms were placed in calculated positions and refined by using a riding model. The final cycle of full-matrix least-squares refinement was based on observed reflections and variable parameters. Crystallographic data for **I** and **II** are given in Table 1. Selected bond lengths and angles are given in Table 2.

Supplementary material for structures **I**, **II** has been deposited with the Cambridge Crystallographic Data Centre (nos. 1409531 (**I**) and 1409531 (**II**); deposit@ccdc.cam.ac.uk or http://www.ccdc.cam.ac.uk).

RESULTS AND DISCUSSION

During the course of construction compound **I**, H_2Cptia underwent decarboxylation and deprotonation to anionic $Ptia^-$. While in compound **II**, H_2Cptia doubly deprotonated to dianionic $Cptia^{2-}$. Obviously, the different conversion modes of the ligand in compound **I** and **II** can be ascribed to the pH value of reaction solution by comparing the reaction condition. Conversion of ligand H_2Cptia during the course of construction of **I** and **II** may be shown as the following:

Table 1. Crystallographic data and structure refinement parameters for **I** and **II**

Parameter	Value	
	I	**II**
Crystal system	Monoclinic	Triclinic
Space group	$C2/c$	$P\bar{1}$
a, Å	25.140(2)	10.271(3)
b, Å	6.477(5)	12.403(3)
c, Å	16.348(14)	21.557(7)
α, deg	90	87.170(5)
β, deg	129.719(7)	83.153(5)
γ, deg	90	65.541(17)
V, Å^3	2048(3)	2481.9(1)
Z	4	2
ρ, mg m^{-3}	1.704	1.841
μ, mm^{-1}	0.907	1.605
F(000)	1084	1408
θ Range for data collection, deg	2.11–27.84	1.80–25.00
R_{int}	0.0312	0.0666
Reflections collected	8228	23064
Indeptndent reflections	2429	8648
Number of refinement parameters	161	769
R_1, wR_2 ($I > 2\sigma(I)$)	0.0362, 0.1082	0.1251, 0.2526
R_1, wR_2 (all data)	0.0422, 0.1110	0.1369, 0.2585
GOOF on F^2	1.164	1.206
$\Delta\rho_{\max}/\Delta\rho_{\min}$, e Å^{-3}	0.706/–0.738	1.824/–0.907

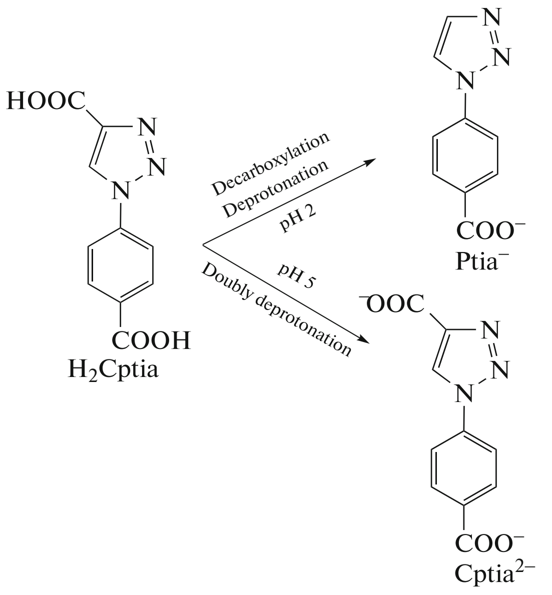

The asymmetric unit of **I** contains half a Co^{2+} ion, one Ptia$^-$ anionic, and two coordination water molecules (Fig. 1). The center Co^{2+} ion is six-coordinated in an elongated octahedral coordination geometry with two N atoms (N(1) and N(2)) from two relevant symmetrical Ptia$^-$. The four O atoms (two O(3) and two O(4)) form water molecules occupied the equatorial position. The carboxyl group of Ptia$^-$ didn't coordinate with any metal centers. The bond length of Co—O(3), Co—N(1), and Co—O(4) is 2.05(16), 2.13(18), and 2.15(16) Å, respectively. The angles around Co(II) center is 86(7)°, 94(7)°, 89(7)°, 91(6)°, and 180(6)°, respectively (Table 2).

In compound **II**, the center Ni^{2+} ion is six-coordinated in an elongated octahedral geometry with one N atom, and two O atoms from two ligands Cptia^{2-}. The other coordination position was occupied by three water molecules (Fig. 2). The dianionic Cptia^{2-} afford one N atom and one carboxyl O atom from the triazol

Table 2. Crystallographic data and structure refinement parameters for **I** and **II***

Bond	*d*, Å	Angle	ω, deg
		I	
Co(1)–O(3)	2.0546(17)	O(3)Co(1)N(1)	85.69(5)
Co(1)–N(1)	2.130(2)	O(3)Co(1)O(4)	88.69(7)
		N(1)Co(1)O(4)	91.31(7)
		N(1)Co(1)O(3)	94.31(5)
		II	
Ni(1)–O(1)	2.022(6)	O(19)Ni(3)N(7)	92.6(3)
Ni(1)–O(6)	2.034(6)	O(16)$^{\#3}$Ni(3)O(20)	91.8(2)
Ni(1)–N(3)$^{\#1}$	2.036(6)	O(19)Ni(3)O(20)	88.4(2)
Ni(1)–O(5)	2.071(6)	N(7)Ni(3)O(20)	95.2(2)
Ni(1)–O(7)	2.104(6)	O(16)$^{\#3}$Ni(3)O(18)	92.1(2)
Ni(1)–O(3)$^{\#1}$	2.107(6)	O(19)Ni(3)O(18)	92.1(2)
O(3)–Ni(1)$^{\#2}$	2.107(6)	N(7)Ni(3)O(18)	80.9(2)
N(3)–Ni(1)$^{\#2}$	2.036(6)	O(20)Ni(3)O(18)	176.1(2)
Ni(3)–O(16)$^{\#3}$	1.989(6)	O(16)$^{\#3}$Ni(3)O(21)	90.7(2)
Ni(3)–O(19)	2.035(6)	O(19)Ni(3)O(21)	174.5(3)
Ni(3)–N(7)	2.038(7)	N(7)Ni(3)O(21)	83.0(2)
Ni(3)–O(20)	2.071(5)	O(20)Ni(3)O(21)	88.7(2)
Ni(3)–O(18)	2.077(5)	O(18)Ni(3)O(21)	90.5(2)
Ni(3)–O(21)	2.154(5)	O(11)Ni(2)N(6)	170.5(3)
O(16)–Ni(3)$^{\#4}$	1.989(6)	O(11)Ni(2)O(13)	92.5(2)
Ni(2)–O(11)	1.997(5)	N(6)Ni(2)O(13)	96.0(2)
Ni(2)–N(6)	2.046(6)	O(11)Ni(2)O(12)	91.9(2)
Ni(2)–O(13)	2.059(6)	N(6)Ni(2)O(12)	92.7(3)
Ni(2)–O(12)	2.060(6)	O(13)Ni(2)O(12)	88.0(2)
Ni(2)–O(8)	2.080(6)	O(11)Ni(2)O(8)	90.6(2)
Ni(2)–O(14)	2.139(6)	N(6)Ni(2)O(8)	80.9(2)
Ni(4)–O(26)	2.027(6)	O(13)Ni(2)O(8)	176.9(2)
Ni(4)–O(23)	2.035(6)	O(12)Ni(2)O(8)	92.6(2)
Ni(4)–O(28)	2.042(6)	O(11)Ni(2)O(14)	91.9(2)
Ni(4)–N(10)	2.053(7)	N(6)Ni(2)O(14)	83.9(2)
Ni(4)–O(27)	2.088(5)	O(13)Ni(2)O(14)	89.3(2)
Ni(4)–O(24)	2.126(5)	O(12)Ni(2)O(14)	175.4(2)
Angle	ω, deg	O(8)Ni(2)O(14)	89.9(2)
O(1)Ni(1)O(6)	87.7(2)	O(26)Ni(4)O(23)	93.0(3)
O(1) Ni(1)N(3)$^{\#1}$	172.8(3)	O(26)Ni(4)O(28)	179.1(3)
O(6)Ni(1)N(3)$^{\#1}$	91.8(2)	O(23)Ni(4)O(28)	86.2(2)
O(1)Ni(1)O(5)	92.4(3)	O(26)Ni(4)N(10)	88.9(3)
O(6)Ni(1)O(5)	179.3(2)	O(23)Ni(4)N(10)	171.5(2)
N(3)$^{\#1}$Ni(1)O(5)	88.2(3)	O(28)Ni(4)N(10)	92.0(3)
O(1)Ni(1)O(7)	90.9(2)	O(26)Ni(4)O(27)	88.9(2)
O(6)Ni(1)O(7)	90.8(2)	N(10)Ni(4)O(27)	98.0(2)
O(1)Ni(1)O(3)$^{\#1}$	92.3(2)	O(26)Ni(4)O(24)	89.9(2)
O(6)Ni(1)O(3)$^{\#1}$	90.6(2)	O(23)Ni(4)O(24)	91.1(2)
N(3)$^{\#1}$Ni(1)O(3)$^{\#1}$	80.5(2)	O(28)Ni(4)O(24)	90.4(2)
O(5)Ni(1)O(3)$^{\#1}$	90.1(2)	N(10)Ni(4)O(24)	80.6(2)
O(16)$^{\#3}$Ni(3)O(19)	94.1(2)		

* Symmetry transformations used to generate equivalent atoms for **II**: $^{\#1}$ $x - 1, y + 1, z$; $^{\#2}$ $x + 1, y - 1, z$; $^{\#3}$ $x, y - 1, z$; $^{\#4}$ $x, y + 1, z$.

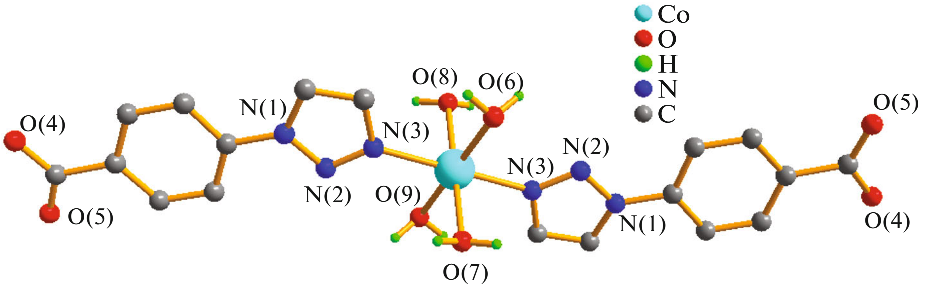

Fig. 1. Local coordination environments of Co(II) in **I** (some H-atoms are omitted for clarity).

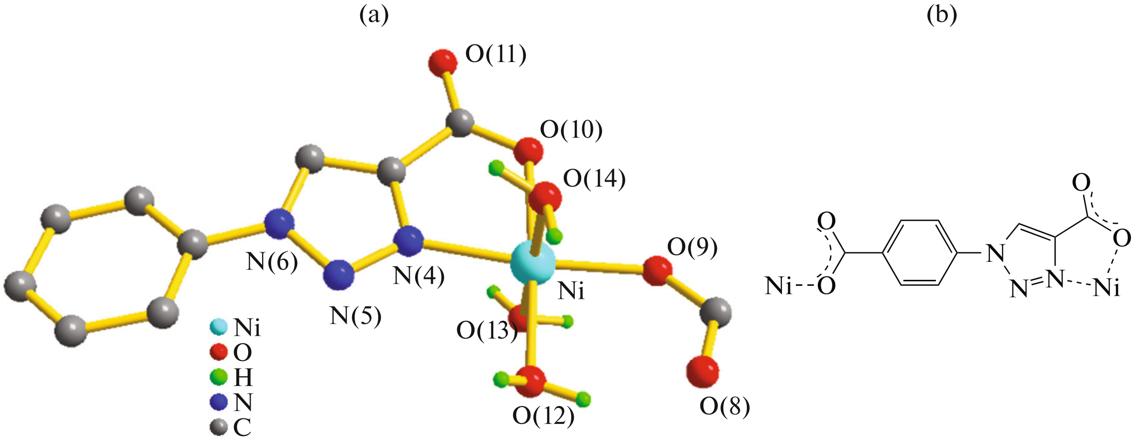

Fig. 2. Local coordination environments of Ni(II) in **II** (some H-atoms are omitted for clarity) (a); bridging Co(II) modes of the ligands Ptia^{2-} in **II** (b).

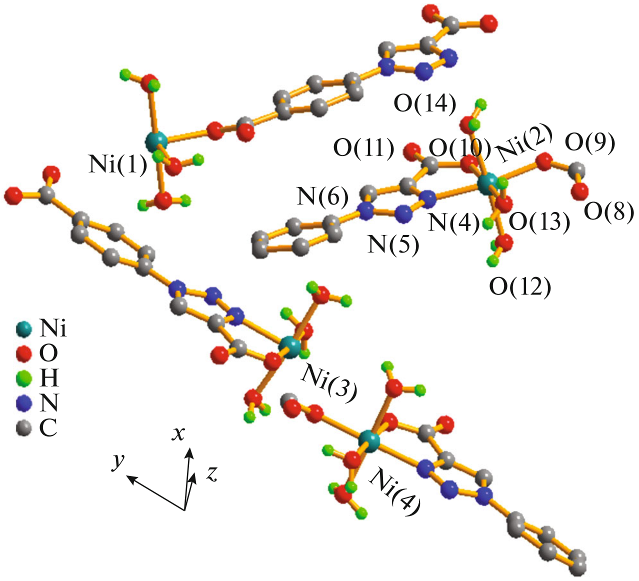

Fig. 3. The composition of one unsymmetrical unit in **II** (some H-atoms are omitted for clarity).

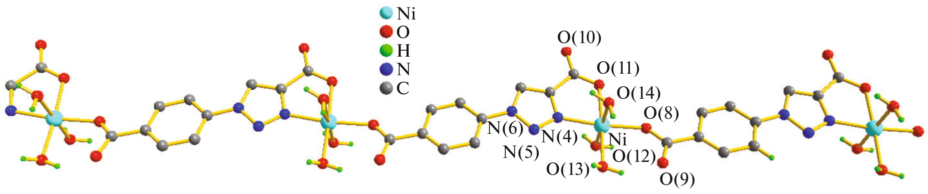

Fig. 4. A schemetic view of the 1D chain in **II** (some H-atoms are omitted for clarity).

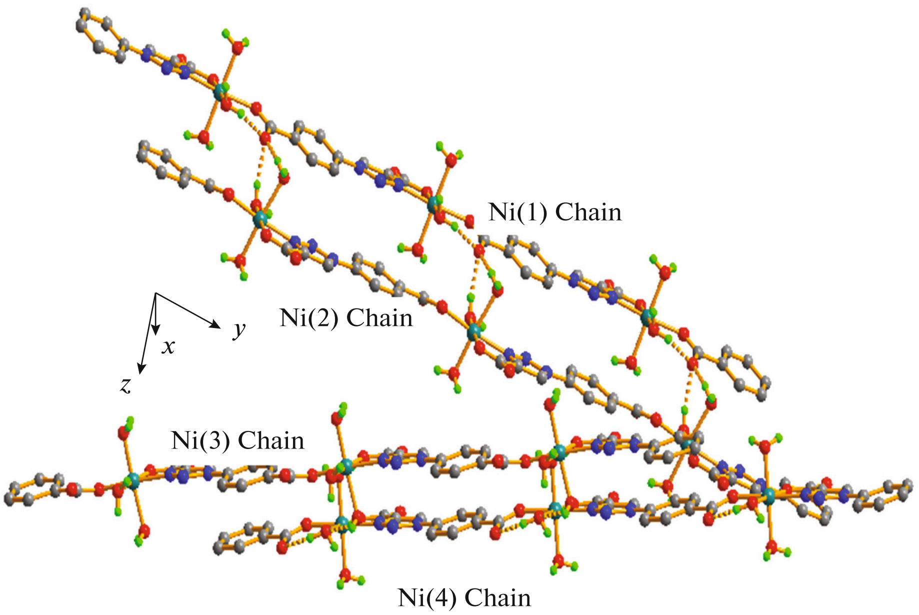

Fig. 5. Four chains orients in different direction in **II** (some H-atoms are omitted for clarity).

ring to chelate with Ni atom and one carboxyl O atom from the benzene ring to coordinate with another Ni atom (Fig. 3) to form 1D chains structure. One asymmetric unit of **II** contains four Ni(II) centers and four Cptia^{2-} with the same coordination modes and the same coordination environment (Fig. 4). Obviously, four Ni(II) centers can form four 1D chains (as designated infra with Ni(1), Ni(2), Ni(3), and Ni(4) chains). These chains orient in different direction in three dimension space (Fig. 5). The Ni(1) chain and Ni(2) chain arrange in parallel due to H-bonds interaction between one non-coordination carboxyl O from Ni(1) chains and one coordination water molecule from the Ni(2) chains. Likewise, Ni(3) chain parallels with Ni(4) chain.

The magnetic properties of **I** and **II** were investigated in the 2.0–300 K range at 1000 Oe. The magnetic susceptibility of **I** versus temperature is shown in Fig. 6a. The $\chi_M T$ value is 3.25 cm^3 K mol^{-1} at 300 K, which is significantly bigger than the spin-only value of 1.88 cm^3 K mol^{-1} calculated for one Co^{2+} ions (S = 3/2, g = 2.0). This may be due to the spin-orbit coupling effect of Co^{2+} ions. With the decreasing of temperature, the $\chi_M T$ decrease. In the temperature range of 60–200 K, the magnetic susceptibility obeys the Curie–Weiss law with Weiss constant, $\theta = -0.0326$ K, and Curie constant, $C = 0.1152$ cm^3 K mol^{-1}. The negative θ value verifies the weak antiferromagnetic interaction among the Co^{2+} ions.

As it can be seen from Fig. 6b, the $\chi_M T$ value of **II** is 1.09 cm^3 K mol^{-1} at 300 K, which is very close to the spin-only value of 1.0 cm^3 K mol^{-1} calculated for (S = 1, g = 2.0). With the decreasing of temperature, the $\chi_M T$ decrease. The observed χ_M^{-1} data of **II** can be roughly fitted to the Curie–Weiss law with C =

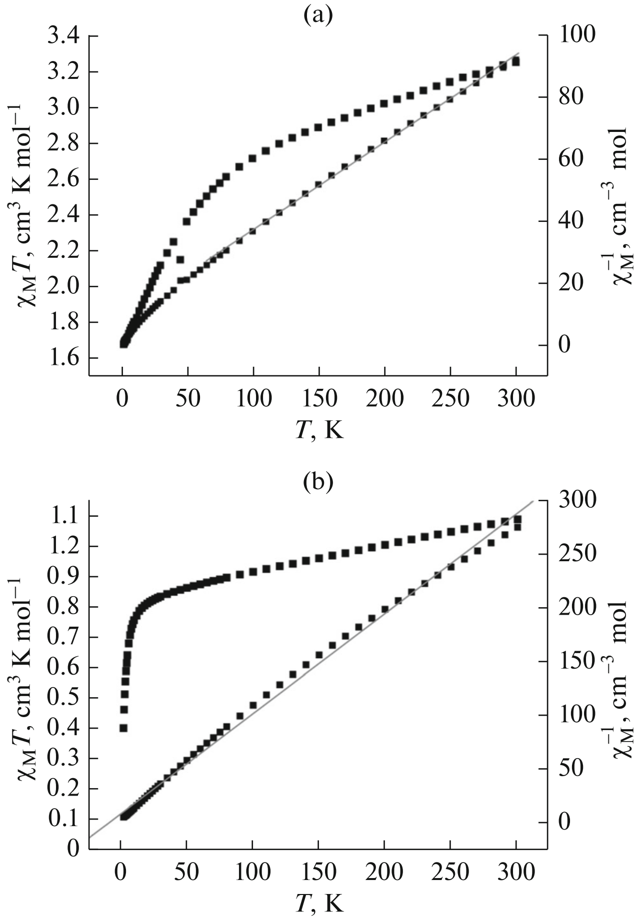

Fig. 6. The $\chi_M T$ and $1/\chi_M$ versus T plots of **I** (a) and **II** (b) (the solid line represents the best fit of Curie–Weiss law).

6.31 cm^3 K mol^{-1}, $\theta = -9.90$ K. The negative θ value verifies the weak antiferromagnetic interaction among the Ni^{2+} ions.

ACKNOWLEDGMENTS

The authors gratefully acknowledge funding from China Scholarship Council (CSC), Innovation and Entrepreneurship Training Program for College Students (X2015020), and the National Natural Science Foundation of China (no. 21371103).

REFERENCES

1. Kurmoo, M., *Chem. Soc. Rev.*, 2009, vol. 38, p. 1353.
2. Palii, A., Tsukerblat, B., Klokishner, S., et al., *Chem. Soc. Rev.*, 2011, vol., 40, p. 3130.
3. Bowman, A., Claridge, J.B., and Rosseinsky, M.J., *Chem. Mater.*, 2006, vol. 18, p. 2046.
4. Pedersen, K.S., Sorense, M.A., and Bendix, J., *Coord. Chem. Rev.*, 2015, vol. 299, p. 1.
5. Sharples, J.W. and Collison, D., *Coord. Chem. Rev.*, 2014, vol. 260, p. 1.
6. Charalambous, M., Moushi, E.E., Papatriantafyllopoulou, C., et al., *Chem. Commun.*, 2012, vol. 48, p. 5410.
7. Tandon, S.S., Bunge, S.D., Rakosi, R., et al., *Dalton Trans.*, 2009, vol. 33, p. 6536.
8. Li, J., Tao, J., Huang, R.-B., et al., *Inorg. Chem.*, 2012, vol. 51, p. 5988.
9. Miyasaka, H., Nezu, T., Sugimoto, K., et al., *Inorg. Chem.*, 2004, vol. 43, p. 5486.
10. King, E.R., Sazama, G.T., and Betley, T.A., *J. Am. Chem. Soc.*, 2012, vol. 134, p. 17858.
11. Ji, J., Wang, G., Wang, T., et al., *Nanoscale*, 2014, vol. 6, p. 9185.
12. Sen, R., Mal, D., Brandao, P., et al., *Cryst. Growth Des.*, 2013, vol. 13, p. 5272.
13. Yuan, F., Shen, S.-S., Hu, H.-M., et al., *Inorg. Chim. Acta*, 2015, vol. 430, p. 17.
14. Monakhov, K.Y., López, X., Speldrich, M., et al., *Chem. Eur. J.*, 2014, vol. 13, p. 3769.
15. Sun, Y.-G. and Wu, Y.-L., Xiong, G., et al., *Dalton Trans.*, 2010, vol. 47, p. 11383.
16. D'Aleo, A., Xu, J., Moore, E.G., et al., *Inorg Chem.*, 2008, vol. 47, p. 6109.
17. Lin, J.-D., Cheng, J.-W., and Du, S.-W., *Cryst. Growth Des.*, 2008, vol. 8, p. 3345.
18. Lu, W.-G., Jiang, L., Feng, X.-L., et al., *Cryst. Growth Des.*, 2006, vol. 6, p. 564.
19. Xie, L.-X., Hou, X.-W., Fan, Y.-T., et al., *Cryst. Growth Des.*, 2012, vol. 12, p. 1282.
20. Yang, Q., Zhao, J.-P., Hu, B.-W., et al., *Inorg. Chem.*, 2010, vol. 49, p. 3746.
21. Sun, Y.-G., Gao, X., Xiong, G., et al., *Inorg. Chim. Acta*, 2014, vol. 409, p. 497.
22. Liao, S.-Y., Gu, W., Yang, L.-Y., et al., *Cryst. Growth Des.*, 2012, vol. 12, p. 3927.
23. Liao, S.-Y., Li, T.-H., Tian, J.-L., et al., *RSC Adv.*, 2014, vol. 56, p. 29877.